Section 3: Report on the project by UR Responsible

3.1 UR information

3.1.1 UR no. 3.13
3.1.2 UR responsible: Zonno Gaetano
3.1.3 Email: zonno@mi.ingv.it

3.2 Activity of UR (1° and 2° year of the project)

The main goal of this Research Unit was to establish a work flow for a multi-layer map that includes (1) the seismicity of Italy in terms of maximum ground shaking, and (2) the near-field/far-field boundaries of the major seismogenic faults.

The Maximum Observable Shaking (MOS) is an the innovative concept of maps. Ground shaking computed for the seismogenic sources included in the DISS database (Fig. 1) is used to determine the potential impact that expected earthquakes might have on all over Italy and offer the civil protection a start up overview of potential seismic hazard over large areas. Having such a regional overview allow decide where strong motion simulations and observation on specific engineering targets need to be investigated in a higher details.

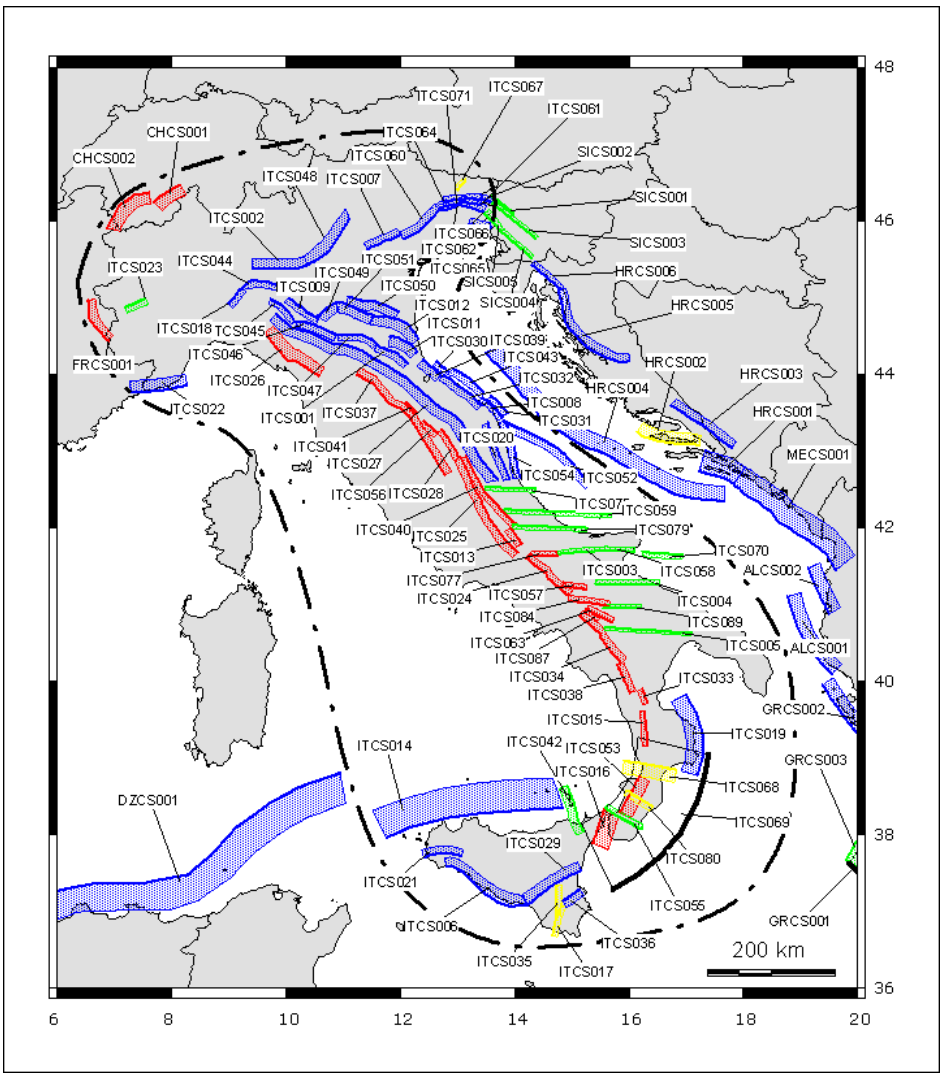

Figure 1. Map of the CSS from the DISS, version 3.1.0 database (DISS Working Group, 2009), classified according to faulting mechanism. Red, normal (NN); blue, reverse (RR); green, right-lateral (RL) strike slip; yellow, left-lateral (LL) strike slip; black, subduction. Bold line, top edge of fault; pattern, vertical projection of fault to ground surface; dashed line, the study area

Our approach relays on the improved understanding of the Italian regional tectonic setting and uses composite seismic sources (CSS) taken from an Italian database of individual seismic sources (Fig. 1). The CSS are merged with the High-Frequency (HF) scenario calculations of expected maximum shaking in a given area. For a given CSS, we consider the associated typical fault, and compute the ground shaking for a rupture model derived from its associated maximum credible earthquake. As the maximum credible earthquake and typical fault 'float' along (Fig. 2) the CSS (i.e. the computational fault plane takes on different spatial positions), the HF ground motion is computed at each point surrounding the given fault, and the maximum from the observable shaking according to that scenario is plotted on the MOS map.

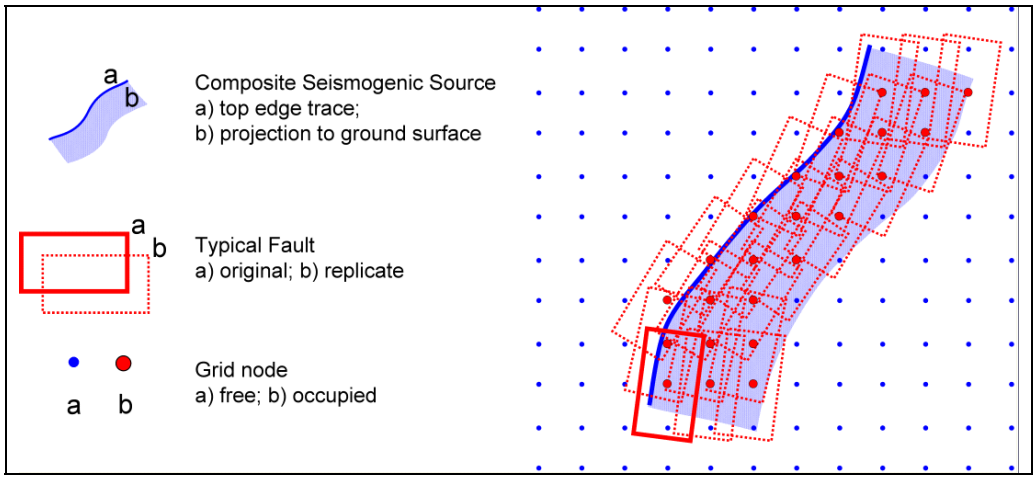

Figure 2 The elements of the procedure for a floating fault along the CSS.

The maximum observable shaking maps

These MOS maps are designed to represent the seismic potential of the Italian region, as derived from a complete knowledge of the seismogenic sources (DISS).

MOS maps are expressed in terms of the ground-motion parameters of PGA (cm/s^2), PGV (cm/s), SI-HI (cm) and SD (cm), and they allow an evaluation of the potential impact of expected earthquakes. This goal can be achieved most efficiently by targeted numerical simulations that cover the parameter range of interest (i.e. in terms of magnitude and distance), and that consider a large suite of earthquake-rupture scenarios.

In the following, we present a general framework for the evaluation of the high-frequency MOS (HF-MOS) maps, as follows:

1. MCE: this is defined for each CSS, and a TF is associated with it. Each CSS includes a number of TFs;
2. Credible rupture parameters: the MCE is modeled according to a rectangular fault plane (i.e. the TF). The rupture model of the TF is defined by a random or Gaussian slip distribution and some other parameters;
3. HF wavefield: computed at all sites within the simulation domain for any given MCE and TF;
4. Ground-shaking computation in terms of PGA, PGV and SI-HI, from the pseudo-velocity response spectra (5% damping) at the site of the simulated time series;
5. MOS map: as the TF floats along and across the CSS, we allow the shake map to 'float' as well, and we pick the maximum shaking at each grid point of the entire simulation domain.

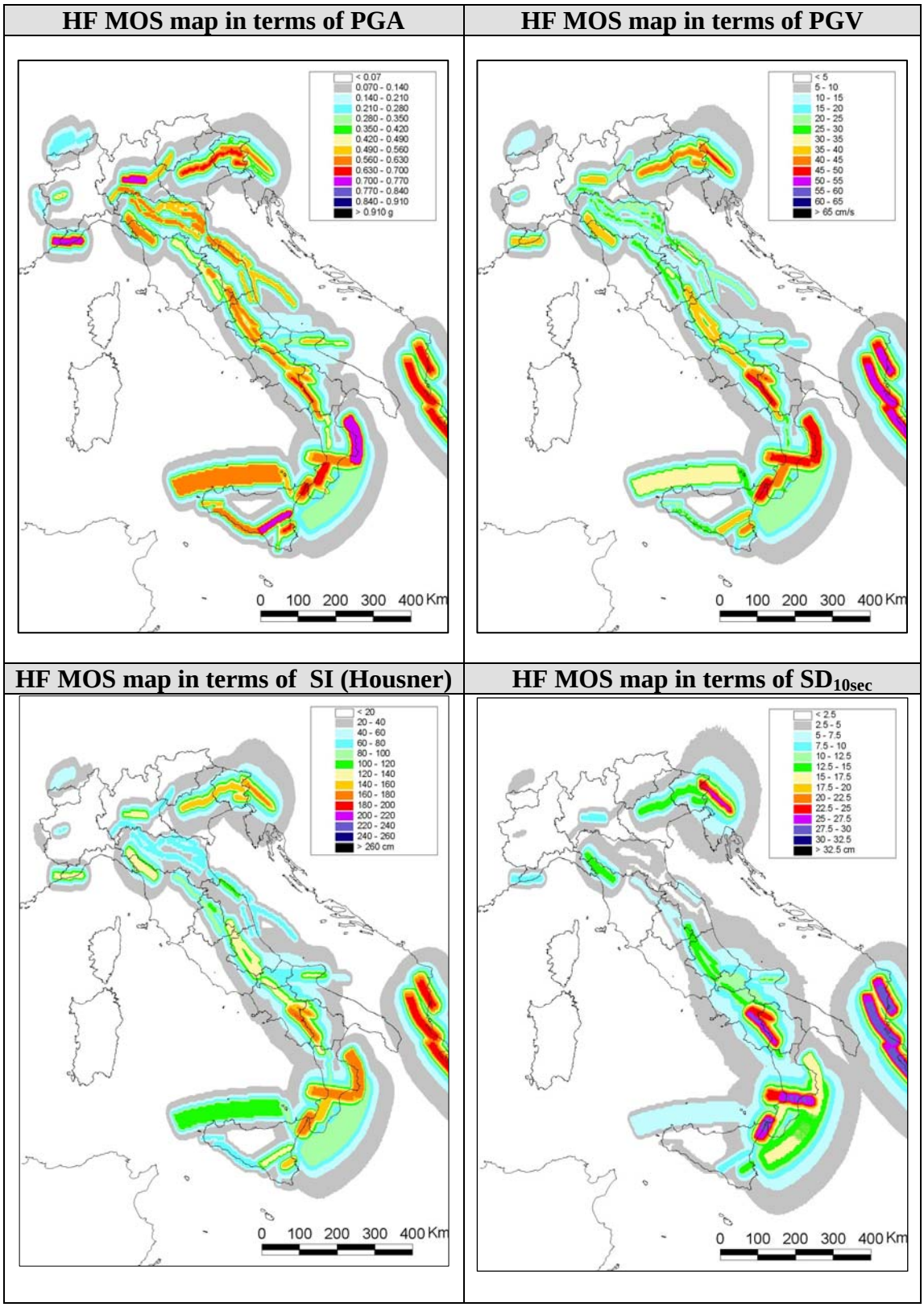

Figure 3. HF MOS maps in terms of PGA (g), PGV (cm/sec), SI-HI (cm) and SD_{10sec} (cm) using the Gaussian slip distribution.

In the analysis, we use bilateral point-of-rupture initiation, considering both random and Gaussian slip distributions. To verify and test our simulated ground-motion predicted against observations, we examine the resulting uncertainties and analyze the variability of ground-motion for a given typical fault using five slip Gaussian distributions, and considering two nucleation points.

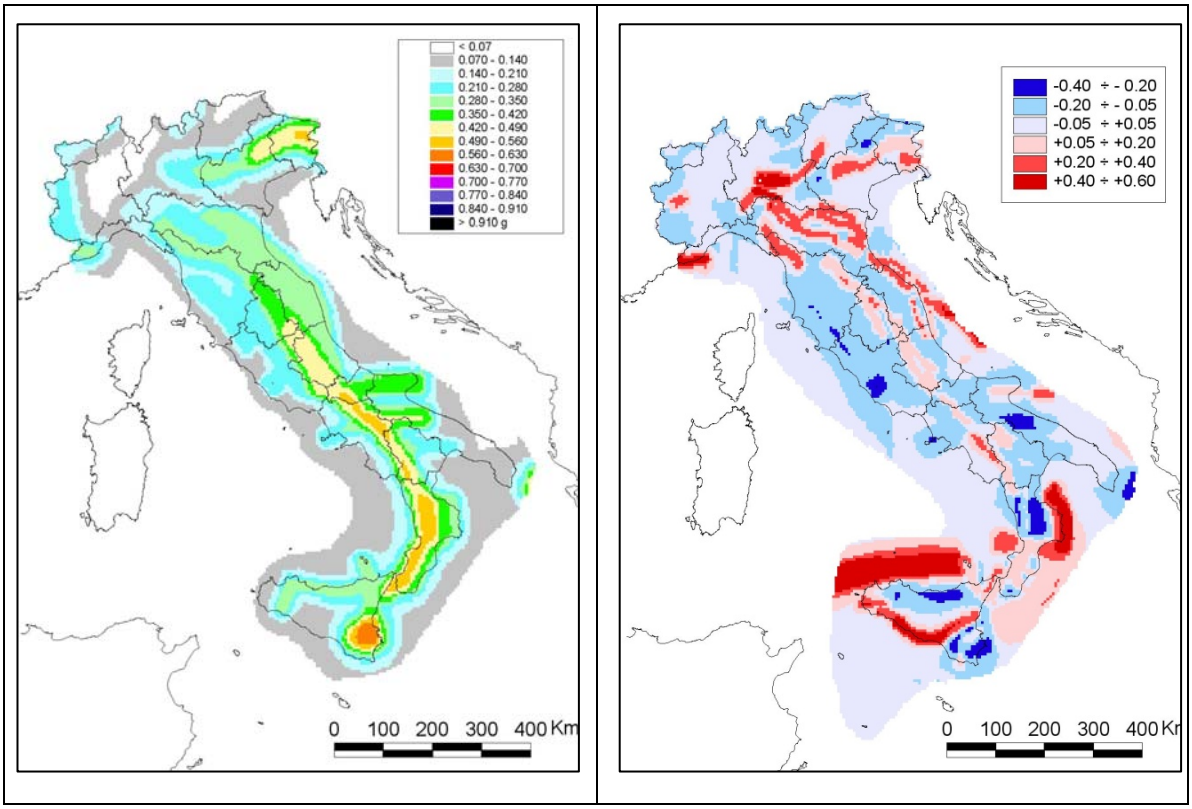

Figure 4. The PGA map (return period 2,475 yr) from MPS04 (left) (Meletti and Montaldo, 2007). The map of the differences of PGA values between the MOS (Gaussian) and MPS04 (right).

The MOS maps need to be compared with observations and/or other independent predictions to confirm their consistency, to verify and 'validate' the results, and to examine their general performance. For this reason, we carried out three main comparisons: (1) the PGA map with the 2% probability of exceedance in 50 years time (return period, 2,475 yr) previously produced for Italy; (2) the results of ShakeMap applied to the L'Aquila earthquake of 6 April, 2009; and 3) the historic felt intensities within the DBMI04 database.

Comparison with the PGA map (return period, 2,475 years)

The results of the MOS of Italy shaking parameters in terms of the PGA were compared with the 2% probability of exceedance in a 50 yr period (MPS04 with return period, 2,475 yr). The comparison is done assuming the hypothesis that the MCEs had the same return period. The PGA values of the MOS are higher in general with respect to the MPS04 PGA map (Fig. 3 and 4). Some of the differences might also arise, as the CSS is in areas where the ZS9 produced low levels of PSH (especially in northern Italy).

We need to consider the comparisons between the MOS in terms of intensity and the maximum felt intensity from DBMI04, as the good results are an indirect validation of the overall procedure of MOS computation.

Furthermore, in terms of intensity, the MOS appears a good tool to investigate the DBMI04 database and to validate the fault source from the shaking point of view.

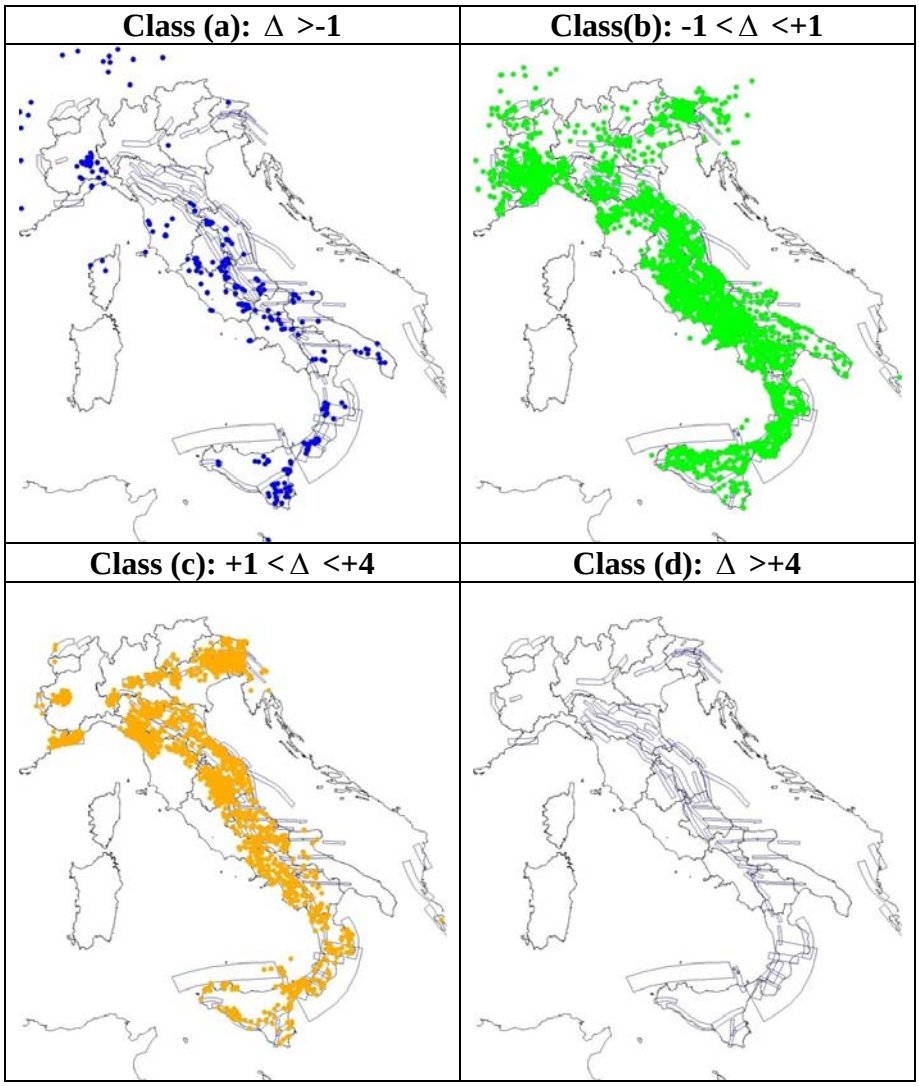

Figure 5. The differences between INT_MOS – DBMI04 (for maximum felt intensity Is ≥6 MCS) are shown spatially distributed into the four classes: (a) Δ **>-1** (blue); (b) **-1** < Δ **<+1** (green); (c) **+1** < Δ **<+4** (orange); and c) Δ **>+4** (red). We note that class C (Δ **>+4)** produces an empty red map.

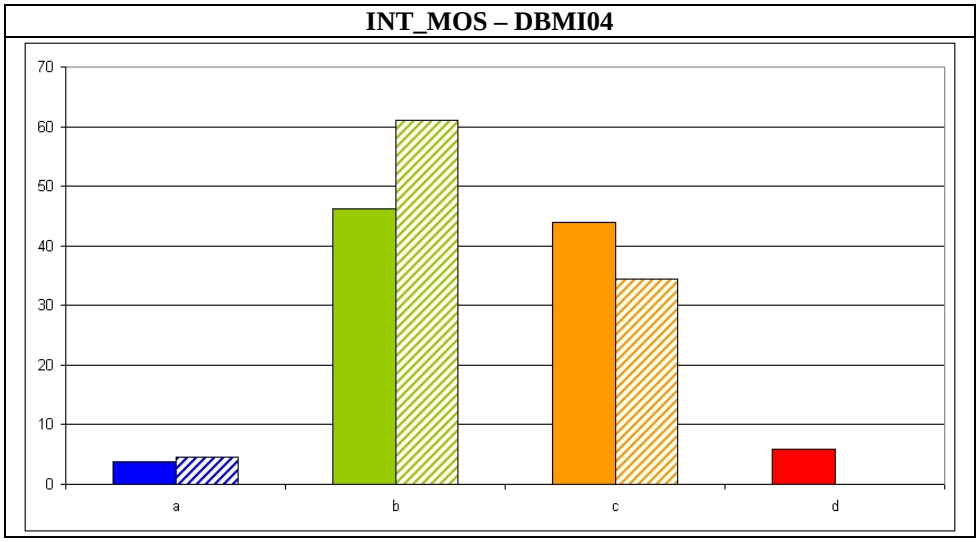

Figure 6. The differences between the INT_MOS and the maximum intensities observed in the DBMI04 database, shown as expressed in percentages for each class for all of the felt intensities (full color) and for the maximum felt intensity Is ≥6 MCS (straight line). The four different classes are: (a) Δ **>-1** (blue); (b) **-1** < Δ **<+1** (green); (c) **+1** < Δ **<+4** (orange); and c) Δ **>+4** (red).

Near-field/far-field boundaries of the major seismogenic faults.
The near-field (NF), Intermediate-Field (IF) and Far-Field (FF) terms represent different properties of the wave-field: the near-source motions are more sensitive to the spatio-temporal details of the rupture process, while far-field terms carry the overall signature of the rupture encoded into the moment-rate function. Although there is no distance at which the NF terms can be completely ignored, the above three terms have different decays:

- NF-waves depend on the temporal slip-evolution on the fault plane, and decay as $1/r^3$ with distance r;
- IF-waves have amplitude and properties depending on the slip function, and decays as $1/r^2$
- FF-waves depend on the slip-rate function and decay as $1/r$.

The FF motions often exhibit peak ground acceleration (*PGA*) within the resonance frequency of buildings, and hence are important for engineering purposes. In this context it is of interest to be able to define the (approximate) region in which NF-radiation needs to be included for accurate shaking-level estimation (and beyond which it is sufficient to only consider the dominating far-field radiation), and where FF-waves dominate.

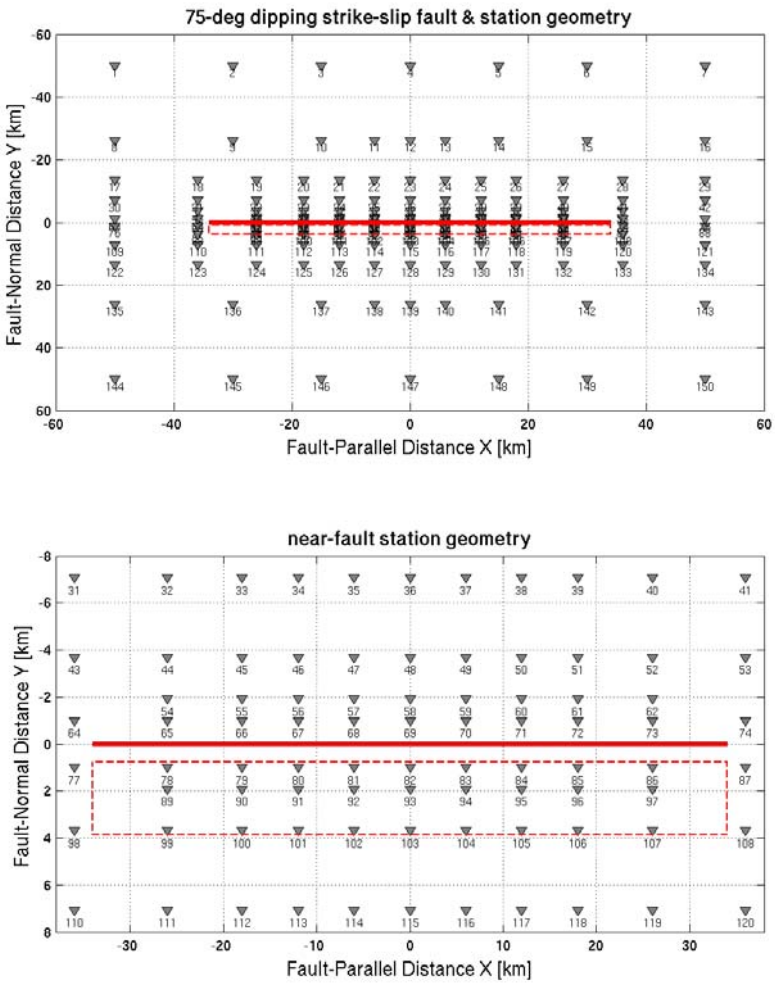

Figure 7. Station geometry used in this study. 150 sites are located at approximately regular inter-station spacing in fault-parallel (X) direction, approximately logarithmically spaced in fault-normal (Y) direction. The sold red line marks the surface-projection of the upper edge of the fault plane, the dotted line shows the projection of the 75°-dipping fault. Top: entire simulation domain; bottom: near-fault region only.

Depending on the particular engineering application and seismic design criteria, it could be sufficient to perform approximate high-frequency far-field ground-motion simulation instead of carrying out expensive full wavefield computations that contain all NF, IF, and FF-terms.

Numerical simulations performed in this study are based on two different finite-fault ground-motion simulation techniques that account for rupture model complexity. Both numerical codes consider 1D layered velocity structures. We compute high-frequency (up to ~10 Hz)far-field (FF) radiation using the ISOSYN package (Spudich&Xu, 2003), for arbitrarily complex source-rupture models. Low frequency ($f \leq 2$ Hz) complete seismograms, containing additionally all NF and IF terms, are computed using the COMPSYN package (Spudich&Xu, 2003), a discrete-wavenumber / finite-element code.

The initial set of simulations (see Report to Phase 1, April 30, 2009) used simplified source models (uniform slip, uniform rise time, and constant rupture speed) to obtain first-order estimates on NF/FF radiation effects. Subsequently we used a variety of faulting styles, fault geometries, and different realizations of heterogeneous slip on the fault and we set the station distribution (Figure 7) to fully include footwall and hanging wall effects as well as capturing a larger distance range. The velocity-density model, roughly corresponding to the structural model for the Colfiorito region, was designed to suppress strong surface-wave contributions, which have been found to dominate over NF/FF effects (see Report to Phase 1, April 30, 2009).

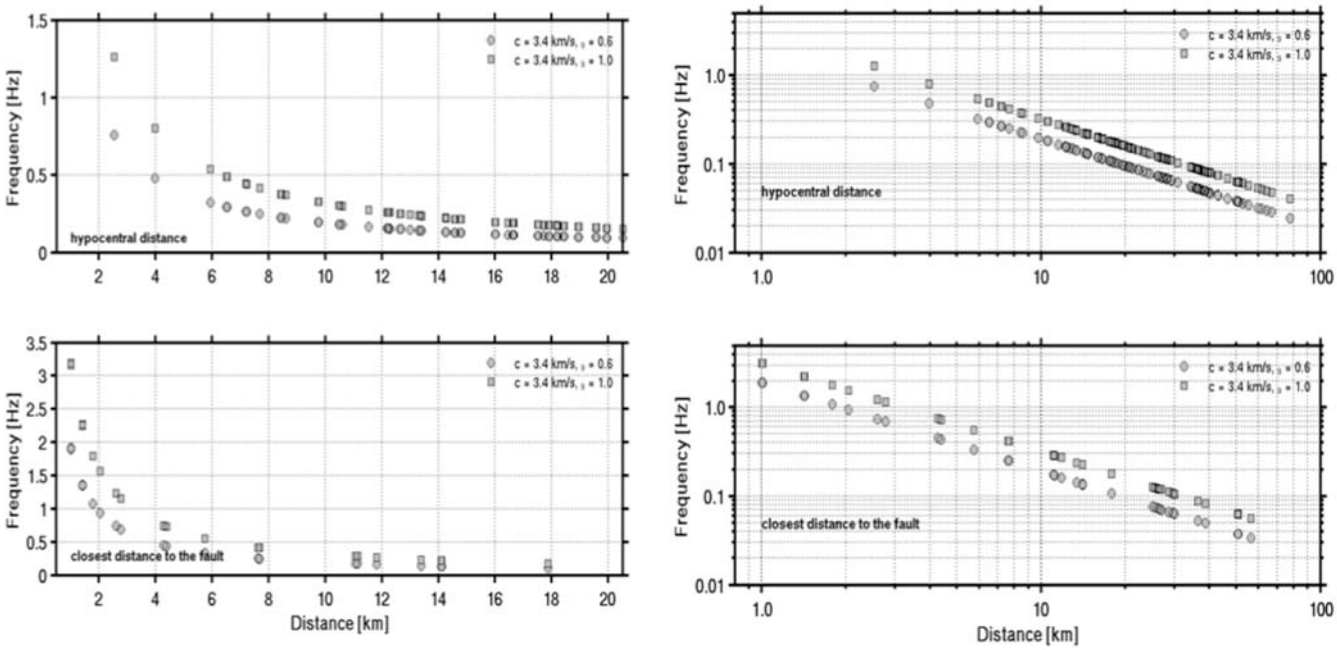

Figure 8. Importance of near-field effects, according to Eq. [1] (Ichinose et al., 2000) for typical distance measures in our study (top panels: hypocentral distance; bottom panels: closest distance to the fault). The left two graphs show the near-source range (0 – 20 km) on a linear-linear scale, the right panels depict the entire distance range of interest on a log-log-scale.

Simplified approach to definition of NF boundary

A simplified study of the NF terms has been carried out by Ichinose et al. (2000) to address the importance of near-field and far-field radiation in layered media for point-source excitation. More specifically, near-field and far-field radiation needs to be treated frequency dependent, in that the far-field terms dominate already at short distances for high frequencies,

while for low frequencies the near-field terms may be important to large distances. This statement can be recast into a dimensionless scalar, valid for a homogeneous half-space (e.g. Madariaga, 2009), that outlines the far-field condition

$$\omega R/c >> 1 \tag{1}$$

In Eq. [1], ω is angular frequency, R is hypocentral distance, and c the corresponding wave speed. Rewriting [1] in terms of wavelengths yields $R/\lambda >> 1$, where $\lambda = 2\pi c/\omega$.
This shows that depending on the frequency content of the signal, we may be in the far-field for high-frequencies at a particular observer location, while for the low frequency wave field the same location experiences near-field effects.
Using Equation [1] and the station geometry for our simulation (Figure 7), we compute a first-order approximation on the distance range where near-field effects are important (Figure 8). Alternatively, the relations can be interpreted in terms of the frequency at which the near-field and far-filed terms converge.

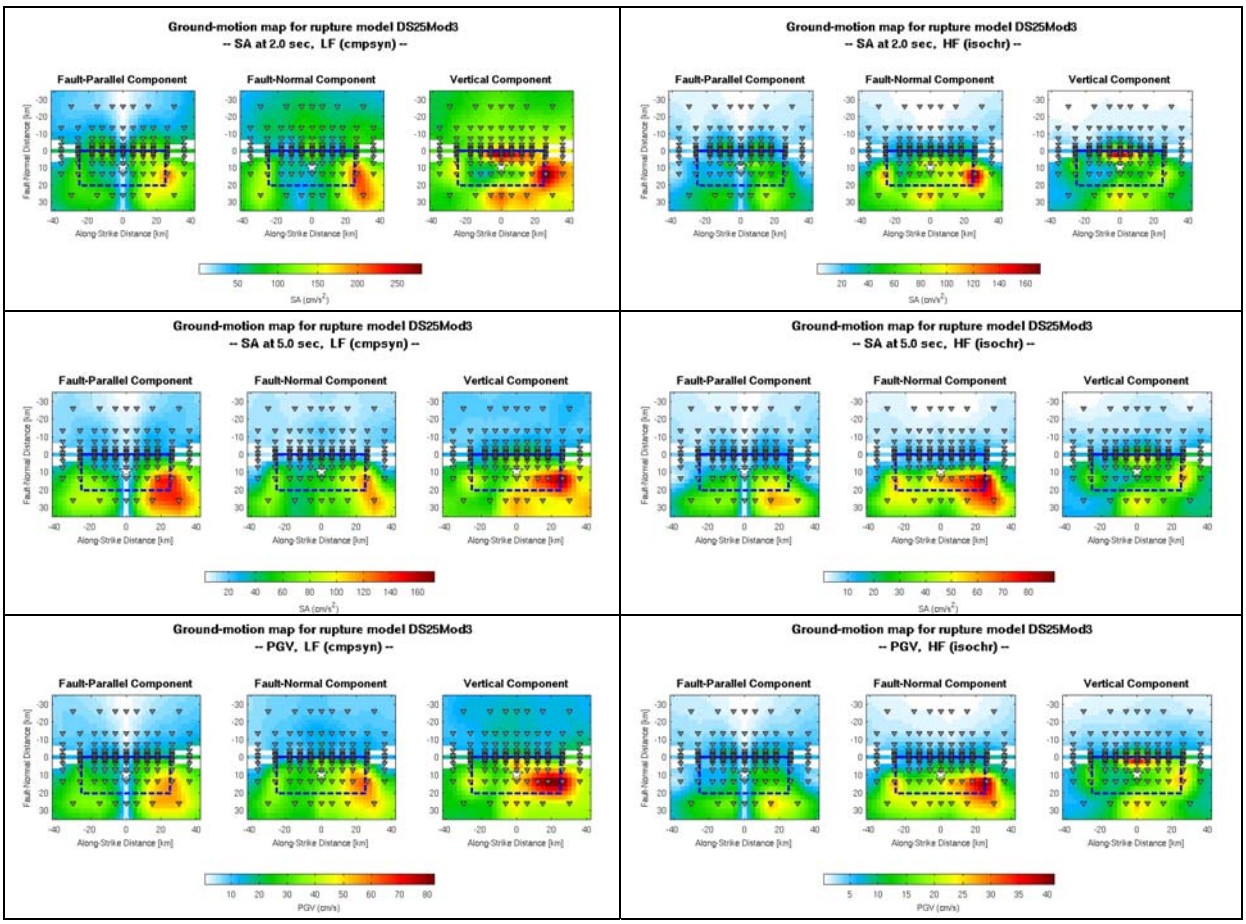

Figure 9. Shake maps to identify near-field effects. A 25° dipping thrust-faulting scenario event DS25Mod3 for T = 2sec (top row), T = 5 sec (center row) and PGV (bottom row), for full-wave field (left column) and far-field (right column) synthetics. For details see Figure 7. Note the similarities in the overall shaking pattern between the two sets of synthetics, but also the differences in the details (particularly in the vertical component and for the footwall stations) due to near-field effects

This model assumes a homogeneous half-space and point-source radiation, and hence cannot be taken literally when considering complex ruptures embedded in layered or even 3D Earth structure. Moreover, this model does not consider the different components of motion – fault-normal, fault-parallel, vertical – onto which that radiated seismic energy is partitioned,

depending on the faulting style. However it gives a rough estimate of the range of frequency and distances at which NF and FF terms are important.

Analyzing our suite of ground-motion simulations for 150 sites in the distance range of ±50 km from a M_w 7.1 scenario event, occurring on a 25°-dipping thrust-fault, a 45°-dipping or 75°-dipping normal fault, or a 75°-dipping strike-slip fault, we come to the following preliminary conclusion which await further detailed quantification:

- The influence of the near-field term on ground-motion intensities is very strong for dip-slip ruptures (normal fault and thrust-faulting in Fig 9), but less so for ruptures on near-vertical strike slip faults;
- The near-field terms are not equipartioned on the two horizontal component of motion, and hence need to be examined independently; they are also strongly developed on the vertical component, in particular for the dip-slip events on dipping fault;
- For thrust and normal-faulting events, the ground-motion intensities on the vertical component are particularly high; hence, any seismic hazard study concerned about the load on the building/structure due to vertically acting forces has to consider vertical motions for the radiated seismic wavefield;
- As the fault-dip becomes shallower, the symmetry of seismic radiation is broken more strongly, and near-field effects are more clearly distinguishable on the footwall and hanging wall sides of the fault (Fig. 9);
- We do not find a significant effect of the velocity-density structure chosen in this study on the near-field terms and/or ground-motion intensities, most likely because none of the selected models is prone to surface-wave generation;
- The distance range in fault-normal direction over which the near-field effects are significant appears to depend on fault dip, in that for steeper dipping faults the range is smaller while the near-field effects are important over a wide region for shallowly dipping faults;
- Examining spectral acceleration at T = [1 2 3 5] sec and PGV, we do not find significant differences in the extent of the near-field region depending on period (or frequency of seismic waves), most likely due to finite-source effects that partially compensate the strict frequency effects of Eq. [1], but possible also because we consider a single magnitude and rise time only (hence limited the potentially radiated frequency spectrum);
- **Based on the shake maps, we conjecture that the spatial extent in fault-normal direction of the near-field affected area is related to fault width (*W*) and fault dip (*δ*); a first-order estimate would be that this length scale is twice the surface-projection of the down-dip extent of the rupture, i.e.**

$$Y_{NF} = 2W \cdot \cos\delta \qquad \textbf{(2)}$$

- No conclusive statements are possible for the along-strike extent of the near-field affected area due to the limited domain size in our simulations;
- Realistic ground-motion simulations have to include near-field effects for any seismic hazard study that is concerned with ground-motion intensity measures (SA, PGV) that are sensitive to seismic waves at frequencies of 2 Hz and below.

Our simulations for examining near-field and far-field effects establish the base reference cases against which refined numerical work could be carried out that includes more complex source models and a wider magnitude range. It is important to avoid a “contamination” of the

spectral-response analysis of near-field terms by later arriving surface waves. This was partially achieved in this study, by avoiding near-surface shallow S-wave velocity layers. However, such layers are important contributors to ground motion complexity and site amplification, and hence should be included in a more comprehensive study on near-field effects. Moreover, refinement of this work requires a thorough analysis of the relative importance of near-field effect, depending on magnitude and source parameters (rupture speed, rise time, slip complexity). Finally, with a database of simulation results for many source models, faulting styles, and velocity models, one should attempt to develop an empirical relation that allows to estimate the "importance range" of near-field effects, based on source parameters (magnitude, distance, faulting style) and the frequency range of interest.

3.2 Relevance for DPC and/or for the scientific community

MOS maps are meant to represent the seismic potential for the Italian region as they are derived from the complete knowledge of the seismogenic sources (the DISS). They offer an overall view on the entire Italy on where a given range of shaking might occur in response of a future earthquake. However, since the concept of MOS maps is a new and innovative approach, the procedure developed here has been applied only to High-Frequency range.

Since several factors, such as directivity and rise-time, cause ground shaking to be substantially different in the extreme NF than at larger distances, the knowledge of the NF/FF boundary is crucial. However, the computation of the entire wave-field in the low-frequency domain can have significant computation costs. In this work, we examine how to potentially derive empirical relations that may allow delineating NF/FF boundaries. If such a boundary can indeed be quantified, even if only approximately, one can choose to simulate ground-shaking for a given type of building or infrastructure, according to whether its location occurs in the NF or FF regime, with respect to a given source, and for a given frequency of interest.

3.3 Changes with respect to the original plans and reasons for it

We had fruitfully reached the goal to deliver the computation of Maximum Observable Shaking (MOS) maps of Italy using a finite-fault stochastic approach.

However we made important changes:

- a general framework to evaluate the MOS map has been formalize only for the HF frequency range but not yet for the complete wavefield broadband simulations
- the single individual source was used for single site analysis or to study specific past earthquake while the Typical Faults have been used in computing the HF MOS map for the entire Italian Territory floating the faults along the Composite Seismic Sources;
- the HF MOS maps are expressed in terms of not only two ground-motion parameters PGA (cm/sec^2) and SI-Housner (cm) but also in PGV (cm/sec) and SD (cm).

The goal of this near-field/far-field boundary study can in fact be adequately be defined. The original project description includes a theoretical/analytical study on this issue, however, we decided to focus on the numerical aspects of this work to gain insight into the NF/FF properties from to potentially derive an application-oriented empirical relations.

3.4 Deliverables

The following deliverables have been compiled at end of the project:

- **Deliverable 1 # A3.13.1-2-3-4-5:** "Maximum Observable Shaking (MOS) maps of Italy (Final report)", 10th June 2010;
- **Deliverable 2 # A3.13.8**: "Delimitation of Near-fields boundaries (Final report)", 10th June 2010;
- **Deliverable 3 # A3.13.6:** "High-Frequency Maximum Observable Shaking Map of Italy from Fault Sources", 10th June 2010.

3.4.1 Cooperation with the others Unit Research in the framework of the project S1

We have interacted with the UR 3.12 (Resp. Vannoli P.; Task C, AU B) having information and data from the DISS 3.0.2 Data base; with the Task B (Resp. Gasperini P.) and with the Task C (Resp. Basili R.). A methodological interaction has been developed with UR 4.0.1 (Resp. Lavecchia G., Task B).

Key publications

Basili R., G. Valensise, P. Vannoli, P. Burrato, U. Fracassi, S. Mariano, M.M. Tiberti, E. Boschi (2008), The Database of Individual Seismogenic Sources (DISS), version 3: summarizing 20 years of research on Italy's earthquake geology, Tectonophysics, 453, 20-43, doi:10.1016/j.tecto.2007.04.014.

Boore, D. M., 2009. Comparing stochastic point- and finite-source ground-motion simulations: SMSIM and EXSIM, Bull. Seism. Soc. Am. Vol. 99, No. 6, pp. 3202–3216, December 2009, doi: 10.1785/0120090056

Lorito, S., Tiberti, M.M., Basili, R., Piatanesi, A., and Valensise, G., 2008. Earthquake-generated tsunamis in the Mediterranean Sea: Scenarios of potential threats to Southern Italy. Jour. Geophy. Res., 113, b01301, doi:10.1029/2007jb004943.

Ichinose, G.A., Goldstein, P., Rodgers, A.J., 2000. Relative importance of near, intermediate and far-field displacement terms in layered Earth synthetic seismogramsm. Bull. Seismol. Soc. Am. 90, 531–536.

Imperatori, W., and P.M. Mai (2009), Broadband Ground Motion Simulations in the Messina Strait Area (Southern Italy): Appraising Strong Motion Variability due to Complexity in Source and Earth Structure, manuscript in preparation

Madariaga, R. (2009). Earthquake source theory, in Treatise on Geophysics, Part 4 (Earthquake Seismology), Editors H. Kanamori and G. Schubert, Elsevier, pp.59-82.Spudich&Xu, 2003

Mai, P.M, and Beroza, G., 2003. A hybrid method for calculating near-source, broadband seismograms: application to strong motion prediction. Physics of the Earth and Planet. Int., 137: 183-199

Meletti C., F. Galadini, G. Valensise, M Stucchi, R. Basili, S. Barba, G. Vannucci, E. Boschi (2008), A seismic source zone model for the seismic hazard assessment of the Italian territory, Tectonophysics, 450, 85-108, doi:10.1016/j.tecto.2008.01.003.

Motazedian, D., Atkinson, G. M., 2005. Stochastic Finite-Fault Modeling Based on a Dynamic Corner Frequency. Bull. Seis. Soc. Am, 95(3): 995–1010.

Spudich, P., and Xu, L., 2003. Documentation of software package COMPSYN and ISOSYN sxv3.11. In: International Handbook of Earthquake and Engineering Seismology CD, IASPEI, Academic Press, 74 pp.

Zonno, G., Musacchio, G., Basili, R., Imperatori, W., and Mai, P. M., 2008. Stochastic and full-wavefield finite-fault round-motion simulations of the M 7.1, Messina 1908 Earthquake (Southern Italy). Abstract presented at the A.G.U. Fall Meeting 2008, San Francisco (CA-USA), December 2008. http://hdl.handle.net/2122/4742

Zonno G., Musacchio G., Meroni F., Basili R., Imperatori W. and Mai P. M., 2009. Deliverable 1 # A3.13.1-2-3-4-5 prepared by UR 3.13 " Maximum Observable Shaking (MOS) maps of Italy (Preliminary -1° phase)", 30th April 2009

Zonno G., Musacchio G., Meroni F., Basili R., Imperatori W. and Mai P. M., 2009. Deliverable 2 # A3.13.8 prepared by UR 3.13 "Delimitation of Near-fields boundaries (Preliminary -1° phase)", 30th April 2009

Zonno G., Musacchio G., Meroni F., Basili R., Imperatori W. and Mai P. M., 2010. Deliverable 1 # A3.13.1-2-3-4-5: "Maximum Observable Shaking (MOS) maps of Italy (Final report)", 10th June 2010

Zonno G., Musacchio G., Meroni F., Basili R., Imperatori W. and Mai P. M., 2010. Deliverable 2 # A3.13.8: "Delimitation of Near-fields boundaries (Final report)", 10th June 2010

Zonno G.,, Basili R., Meroni F., Musacchio G., Mai P. M., and Valensise G., 2010. Deliverable 3 # A3.13.6: "High-Frequency Maximum Observable Shaking Map of Italy from Fault Sources", 10th June 2010.